Schweizerische Eidgenossenschaft
Confédération suisse
Confederazione Svizzera
Confederaziun svizra

Eidgenössisches Departement für
Umwelt, Verkehr, Energie und Kommunikation UVEK

Bundesamt für Energie BFE

Final Report 23. November 2011

go.PEF-CH

Enhancing PEFC Durability and Reliability under Application-Relevant Conditions

Auftraggeber:
Bundesamt für Energie BFE
Forschungsprogramm Brennstoffzellen
CH-3003 Bern
www.bfe.admin.ch

Auftragnehmer:
Paul Scherrer Institut
CH-5232 Villigen
www.psi.ch

Autoren:
Dr. Lorenz Gubler, PSI, lorenz.gubler@psi.ch
Dr. Nicolas Linse, PSI
Dr. Steffen von Dahlern, PSI
Dr. Michael Höcke, HTI Biel

BFE-Bereichsleiter: Dr. Stefan Oberholzer
BFE-Programmleiter: Dr. Stefan Oberholzer
BFE-Vertrags- und Projektnummer: SI/500095 / SI/500095-01

Abstract

In the go.PEF-CH project, involving the two Swiss industrial partners CEKAtec AG (Wattwil SG) and MES S.A. (Stabio TI), we a) develop the necessary diagnostic tools to investigate transients occurring during non-steady state operation of a polymer electrolyte fuel cell (PEFC), b) measure and quantify respective transients and degradation in custom-built cells as well as technical cells, and c) identify and implement mitigation strategies to improve fuel cell lifetime under application-relevant conditions. We have gained fundamental insights into the local current distribution via the measurement of local currents and the distribution of liquid water using neutron radiography, both in hardware supplied by MES and in-house built model cells. Key results are the mapping of current density along the channels of the flow field (scale: cm to tens of cm) and on the scale of channels and lands (sub-mm resolution). For the latter, a unique 1 cm2 cell with micro-flow field was developed and built at PSI. Key transients that were resolved are short-circuiting of the cell, which is used in the fuel cell systems of MES S.A. to provide intermittent humidification, and start-stop procedures. An implication of using a channel and land geometry for reactant distribution are diffusion limitations. We show that a small differential pressure between adjacent cells significantly improves current generation under the land. This insight can be used to improve the flow field of the fuel cell. The analysis of the short-circuit effects on possible aging of the MEA could not be fully completed and may require additional work for quantification of the degradation phenomena. The start-stop induced degradation of PEFCs was investigated comprehensively on all levels of complexity in single cells and stacks, ranging from fundamental investigations in single cells under controlled potential conditions to start-stop cycling in a 30-cell stack. Based on the analysis of important influencial parameters (humidity, auxiliary resistance, etc.), application-relevant start stop protocols were implemented. In the stack, a distinct influence of the position of individual cells in the stack on the rate of degradation as a result of start-stop cycling was identified. This is a result of the non-ideal distribution of gas during start-up and shutdown. Further work may be necessary to address these inhomogeneities on the stack level.

Project Objectives

The market introduction of products based on the polymer electrolyte fuel cell (PEFC) technology is limited to a large extent by the **aging** and **premature failure** of the electrochemical components and lack of reliability. The objective of this project is to **investigate aging and degradation phenomena** in the form of 2 PhD theses in close collaboration with the industrial partners **CEKA Elektrowerkzeuge AG & Co. KG** (Wattwil, SG) and **MES S.A.** (Stabio, TI).

Major factors limiting durability under application-relevant conditions are rapid **transients** (changes in load) and **start-stop cycles**. Novel diagnostic tools under development at PSI will provide insight into aging phenomena of membrane and electrodes and failure mechanisms and their dependence on operating strategies in single cells and stacks, with experimental support by the 'Berner Fachhochschule für Technik und Informatik (BFH-TI)'. The insights gained will enable the improvement of the **operating strategy**, cell components and design, giving the industry partners key knowledge to allow certification of their PEFC stacks and systems with respect to lifetime.

The objectives for the year 2010 were to deepen the understanding of start-stop induced carbon corrosion, in particular to understand whether and to what extent platinum catalyzes carbon oxidation. In addition, *post mortem* tests were envisaged to qualitatively and quantitatively assess the structural changes in the cathode catalyst layer as a result of carbon loss. Furthermore, the micro-structured cell introduced 2009 was used to investigate sub-millimeter resolved currents on the channel-and-land scale during fuel cell start-up and shut-down.

Project Outline

The project is divided into two sub-projects: With the industrial partner 'CEKA Elektrowerkzeuge' and the 'Berner Fachhochschule für Technik und Informatik (BFH-TI)' the understanding of start-stop induced fuel cell performance degradation is investigated. A dedicated start-up and shut-down strategy is required to minimize aging of the electrochemical components of the cell, notably the cathode catalyst layer. In the second sub-project, transient operation, such as rapid load changes and start/stop operation is investigated using spatially-resolved diagnostic tools developed in-house. The measurement of currents on a sub-millimeter scale is an approach unique in the community and can provide novel insights into local inhomogeneity phenomena.

Summary of Results

START / STOP INDUCED DEGRADATION PHENOMENA

Typically, fuel cell shut-down is performed by purging the hydrogen filled anode compartment with air. To restart the fuel cell, hydrogen is again fed to the anode. During these purging processes, the coexistence of hydrogen and oxygen at the negative electrode leads to the development of potentials exceeding 1 V in certain areas of the positive electrode [1]. These elevated potentials can cause two degradation processes which are highly detrimental to the cathode catalyst layer. First, the pronounced platinum oxide formation can significantly accelerate the electrochemical dissolution of the platinum catalyst. The resulting reduction of active catalyst surface area by Ostwald ripening and diffusion of platinum ions into the ionomer phase leads to increased kinetic losses, thus lowering the performance of the fuel cell. Second, potentials exceeding 1 V can cause severe corrosion of the porous network of carbon particles acting as support material for the fuel cell catalyst (cf. Equation 1). The resulting decrease in cell performance is usually ascribed to a strong decline in mass transport properties, which arises from substantial changes in the catalyst layer morphology [2].

$$C + 2H_2O \rightarrow CO_2 + 4H^+ + 4e^- \quad (1)$$

Since the oxidation of carbon results in the formation of CO_2, catalyst support corrosion can be directly monitored by determining the carbon dioxide concentration in the exhaust gas of the positive electrode. Based on this measurement principle, an experimental procedure was developed which allows a reliable quantification of carbon corrosion under various operating conditions. Initially, this method was used to investigate fundamental corrosion processes occurring under different potential conditions. To enable a reliable control of the driving force leading to carbon corrosion at the positive electrode, the elevated potentials developing during start-up and shut-down of the fuel cell were thereby typically simulated by applying single triangular potential sweeps to cells operated in H_2/N_2 mode. Subsequently, the effect of important operating parameters on start/stop induced degradation behaviour was systematically investigated both under controlled potential conditions in H_2/N_2 mode and dur-

ing real start-up and shut-down processes by purging of the anode compartment with hydrogen and air, respectively. Moreover, the structural changes leading to fuel cell performance loss were analysed by a 3-dimensional microscopy technique (FIB/SEM serial sectioning). Based on the obtained results, operation strategies can be developed which mitigate start/stop induced fuel cell performance loss.

Investigations on fundamental corrosion processes

Since the analysis of carbon corrosion behaviour is based on monitoring the CO_2 concentration in the exhaust gas of the positive electrode, the understanding of the processes leading to carbon dioxide formation under different potential conditions is a prerequisite for all further investigations. To identify the decisive mechanism, CO_2 evolution was therefore systematically determined in response to single potential sweeps applied to cells operated in H_2/N_2 mode. Measurements with different upper and lower limits revealed that CO_2 can be generated in four distinct potential ranges. Besides the corrosion of carbon at potentials exceeding 1 V (Peak II in Figure 1), considerable amounts of CO_2 were found to evolve under potential conditions typically occurring during ordinary fuel cell operation (U_{cell} < 1 V). During the anodic scan of the applied potential sweep, CO_2 formation at approximately 0.55 V can be ascribed to electrooxidation of previously adsorbed carbon monoxide (Peak I). Measurements with different electrode materials and gas compositions suggest that the CO molecules, at least partially, originate from impurities in the reactant gases. Consequently, CO_2 evolution in this potential range can be assumed to be a secondary effect, which does not directly indicate corrosion of the catalyst support material. The formation of carbon dioxide at approximately 0.8 V during the cathodic scan was found to originate from the reaction of carbon surface oxides with catalytically active OH species formed on the platinum particles during the reduction of platinum oxide (Peak III). Finally, CO_2 evolution was detected after decreasing the potential from values exceeding 1 V to values below about 0.6 V (Peak IV). Experiments with different upper and lower potential limits indicate that CO_2 formation in this potential range is based on chemical oxidation of carbon species by hydrogen peroxide. In summary, the results show that carbon corrosion in the potential range below 1 V can considerably contribute to total CO_2 evolution under certain potential conditions. The influence of these corrosion processes on fuel cell performance loss during long-term operation, however, is still unclear.

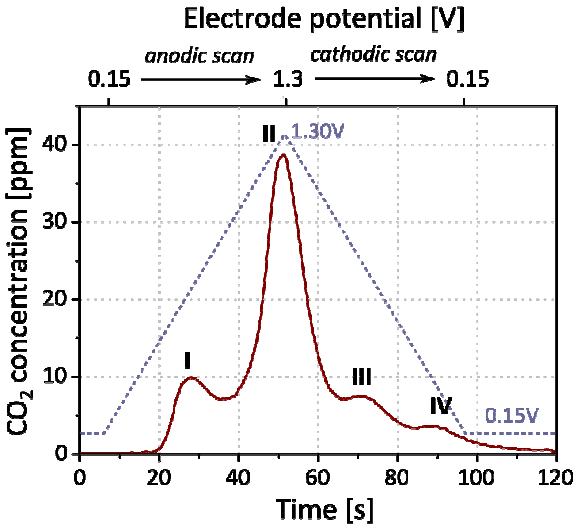

Figure 1 CO_2 evolution at the positive electrode (solid line) during the application of a potential sweep between 0.15 V and 1.3 V (dashed line) to a cell operated in H_2/N_2 mode (80℃, 100% R.H.).

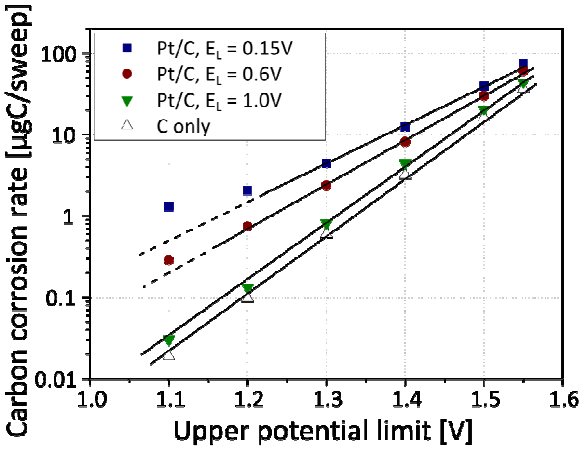

Figure 2 Carbon corrosion rates as a function of the upper potential limit for measurements carried out with different lower potential limits E_L. (80℃, 100% R.H.). The corrosion rates were calculated by integration of CO_2 concentration peaks occurring in response to the application of single triangular potential sweeps to cells operated in H_2/N_2 mode.

As a second fundamental process, the catalytic effect of platinum on the corrosion of the carbon catalyst support material was investigated by applying potential sweeps to fuel cells having electrodes with different Pt/C compositions. The resulting CO_2 concentration peaks in the exhaust gas of the positive electrode were integrated to calculate the carbon corrosion rates. Measurements in various potential ranges showed that the contribution of the platinum catalysed reaction pathway strongly depends on

both the upper and the lower limit of the applied potential sweep. While a decrease in the upper potential limit generally increases the fraction of CO_2 evolved via the catalysed corrosion pathway, two effects of the lower limit were identified [3]. First, in case of lower potential limits exceeding about 0.8 V, the incomplete reduction of platinum oxide leads to the gradual formation of a passivating oxide layer on the platinum particles. Due to the resulting inhibition of the catalysed reaction pathway, the corrosion behaviour determined for a lower limit of 1.0 V is similar to that observed for an electrode which only contains the carbon catalyst support particles and the ionomer (cf. Figure 2). Second, changes in the carbon surface oxide composition caused by an intermittent reduction of quinone to hydroquinone at approximately 0.55 V [4] are suggested to increase the amount of easily oxidisable carbon species. Consequently, a decrease in the lower limit from 0.6 V to 0.15 V additionally promotes the catalysed corrosion pathway (cf. Figure 2).

Depending on the potential conditions and the catalyst loading of the investigated electrode, the presence of platinum was found to increase the carbon corrosion rates by more than one order of magnitude. This substantial catalytic effect of platinum indicates that corrosion induced fuel cell performance loss occurring as result of frequent start-up and shut-down processes can be strongly influenced by the simultaneous decrease in platinum surface area. The results furthermore demonstrate that carbon corrosion is a highly dynamic process, which is markedly influenced by the potential conditions prior to the exposure of the electrode to elevated potentials. Potential hold experiments, which are frequently employed to investigate start/stop induced degradation processes, are therefore not suitable to assess the stability of electrode materials against carbon corrosion.

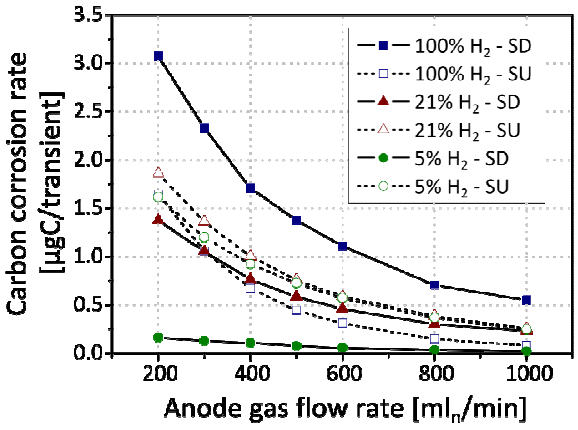

Figure 3 Carbon corrosion rates determined for start-up (SU) and shut-down (SD) processes as a function of the anode gas flow rate for measurements carried out with different hydrogen concentrations. The oxygen concentration was 21% in all cases (50°C, 70% R.H.).

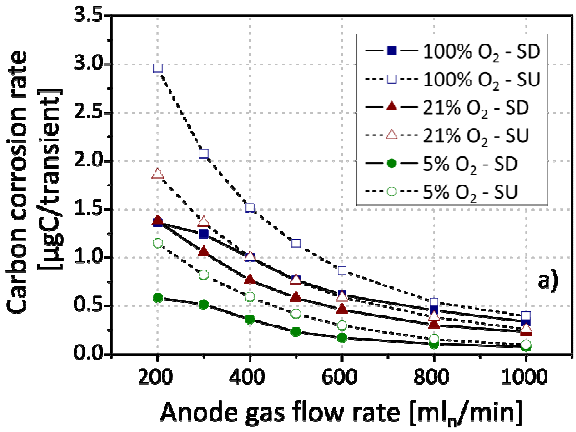

Figure 4 Carbon corrosion rates determined for start-up (SU) and shut-down (SD) processes as a function of the anode gas flow rate for measurements carried out with different oxygen concentrations. The hydrogen concentration was 21% in all cases (50°C, 70% R.H.).

In addition to the measurements carried out under controlled potential conditions in H_2/N_2 mode, the mechanisms related to the exchange of the anode gas were investigated by analysing the carbon corrosion behaviour in response to real start-up and shut-down transients. Since the duration of the detrimental potential conditions is determined by the coexistence of hydrogen and oxygen at the negative electrode, CO_2 evolution rates were found to strongly increase with decreasing anode gas flow rate. Moreover, besides this effect of gas front velocity, carbon corrosion behaviour is also significantly influenced by the composition of the reactant gases. The amount of CO_2 evolved during fuel cell start-up is thereby mainly controlled by the oxygen concentration while the effect of hydrogen content is more pronounced in case of fuel cell shut-down (cf. Figures 3 and 4). This strong influence of reactant gas concentration can be explained by the effect of hydrogen and oxygen which might be trapped in the electrode after the propagation of the gas front through the anode compartment. In case of fuel cell shut-down, the duration of the detrimental potential conditions is controlled by the time necessary to completely remove the hydrogen from the negative electrode. Since this gas replacement process depends on the initial amount of hydrogen, the use of diluted hydrogen results in markedly lower carbon corrosion rates. The influence of oxygen concentration is assumed to be based on a similar effect. However, since carbon corrosion is limited to areas in which both electrodes are filled with (diluted) oxygen, the effect of small residual amounts of oxygen is less pronounced than in case of trapped hydrogen.

The effect of operating parameters on start/stop induced fuel cell degradation

The development of operating strategies which can mitigate start/stop induced fuel cell performance loss requires a profound understanding of the parameters influencing electrode degradation at elevated potentials. Therefore, the effect of important operating parameters was systematically determined on different levels of complexity, ranging from the investigation of single transients under controlled potential conditions to the analysis of fuel cell degradation behaviour during start/stop cycling [5, 6].

The measurements showed that carbon corrosion basically follows the theoretically expected behaviour if the elevated potentials occurring during fuel cell start-up and shut-down are simulated by applying potential sweeps to cells operated in H_2/N_2 mode. While CO_2 evolution rates increase exponentially with increasing potential, reactant gas humidity and temperature variation experiments yielded a linear and Arrhenius-like correlation, respectively. In case of real fuel cell start-up and shut-down, however, the higher complexity of the involved processes can lead to significant deviations from the corrosion behaviour observed under controlled potential conditions. Besides the effect of temperature and humidity on the potential acting as driving force for carbon corrosion at the positive electrode, CO_2 evolution during purging of the anode compartment with hydrogen and air can be influenced by additional phenomena. At high temperatures, for instance, the corrosion rates determined during single start-up and shut-down transients are markedly lower than expected from the exponential-like Arrhenius correlation (cf. Figure 5). This phenomenon can be explained by the expansion of the reactant gases and the increasing fraction of water vapour with increasing temperature. The resulting increase of the effective gas flow rate causes a faster exchange of the anode gas, thus leading to comparatively low carbon corrosion rates. In case of real start/stop processes, an increase in temperature from 40℃ to 90℃ increases the overall carbon corrosion rate by a factor of 3.5 while the same temperature change under controlled potential conditions leads to an increase in CO_2 evolution by a factor of more than 20. Moreover, the propagation of the hydrogen/air front through the anode compartment can be influenced by flooding of the electrode with liquid water. If the cell is operated with fully humidified gases, this effect was found to cause strong deviations from the linear correlation between reactant gas humidity and carbon corrosion rate, which was obtained under controlled potential conditions.

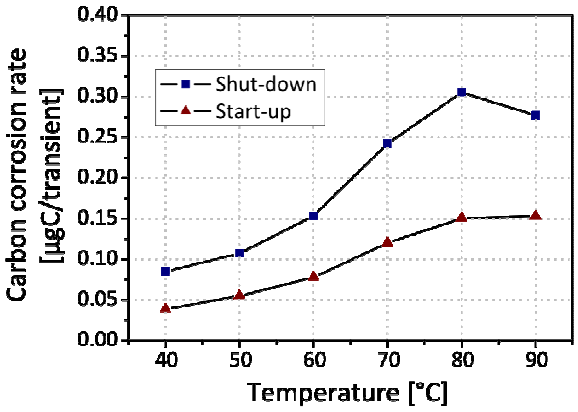

Figure 5 Carbon corrosion rates determined in response to single start-up and shut-down transients as a function of temperature (70% R.H., gas flow rate: 600 ml_n/min, external load: 3 Ωcm^2).

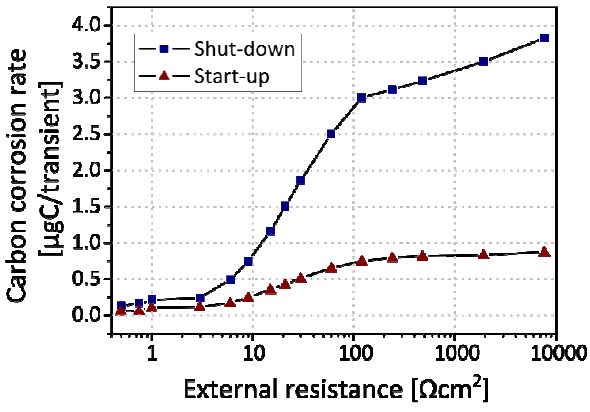

Figure 6 Carbon corrosion rates determined in response to single start-up and shut-down transients as a function of the external resistance (80℃, 70% R.H., gas flow rate: 600 ml_n/min).

Due to the strong influence on the potential developing at the positive electrode, carbon corrosion behaviour is also strongly affected by the external load applied to the cell during start-up and shut-down transients. As shown in Figure 6, resistance values smaller than about 6 Ωcm^2 lead to very similar carbon corrosion rates. This small effect of the applied load might be explained by a comparatively large contribution of CO_2 evolution processes in the potential range below 1 V (cf. Figure 1). If the applied resistance is further increased, the increasing potentials developing at the positive electrode during purging of the anode compartment result in significantly higher carbon corrosion rates. Yet, since the influence of the external load on the detrimental potentials decreases in case of high resistance values, the increase in corrosion rates becomes less pronounced if the load exceeds approximately 100 Ωcm^2.

Besides the investigation of CO_2 evolution in response to single potential sweeps and single start-up and shut-down transients, the effect of operating parameters on start/stop induced performance loss behaviour was systematically analysed by exposing fuel cells to 1,800 start/stop cycles. The measurements showed that the effect of humidity, temperature and external load on the performance loss behaviour is in good agreement with the correlations between the respective parameters and the carbon corrosion rates obtained during the analysis of single start/stop transients. This similar behaviour strongly indicates that the decrease in active platinum surface area only plays a minor role with respect to fuel cell performance loss. Under most operating conditions, the decrease in fuel cell performance can therefore be assumed to be primarily controlled by corrosion induced degradation processes.

The origin of start/stop induced fuel cell performance loss

To obtain further insights into the origin of start/stop induced performance loss, pristine and degraded electrodes were investigated by FIB/SEM serial sectioning. This 3-dimensional microscopy technique allows a quantitative determination of changes in the porous structure of the catalyst layer [7]. Together with additional electrochemical measurements, the images confirm that the decrease in electrochemically active platinum surface area only slightly contributes to the decline in fuel cell performance. The main fraction of voltage loss appears to be based on dramatic changes in the morphology of the catalyst layer. As shown in Figures 7 and 8, start/stop induced corrosion of the carbon structure leads to a substantial loss in catalyst layer porosity. Moreover, the images reveal a strong decrease in average pore size and in the fraction of interconnected pores.

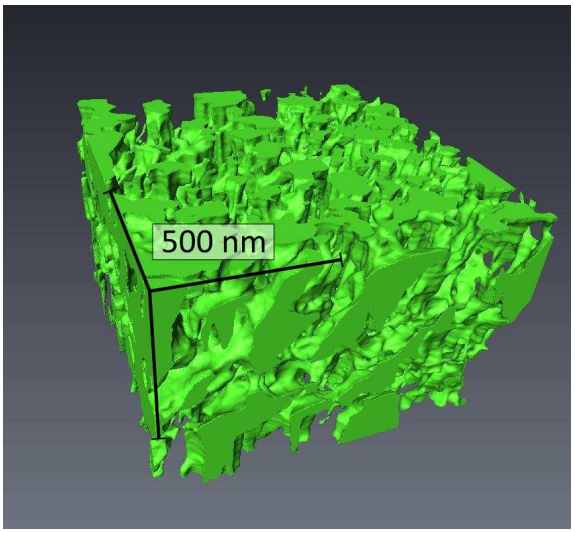

Figure 7 Three-dimensional pore structure of the pristine catalyst layer. The structure was calculated based on several hundred SEM images obtained by FIB/SEM serial sectioning.

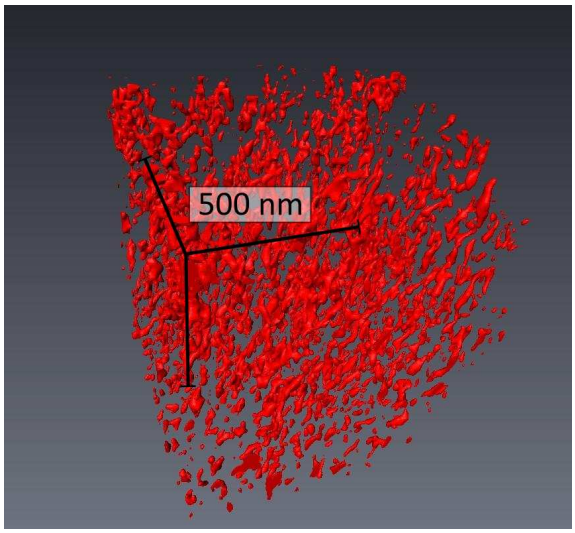

Figure 8 Three-dimensional pore structure after exposure of the fuel cell to 1,000 start/stop cycles by alternating purging of the anode compartment with hydrogen and air. The structure was calculated based on several hundred SEM images obtained by FIB/SEM serial sectioning.

The combined electrochemical and microscopic analysis of degraded electrodes shows that start/stop induced performance loss cannot be ascribed to one specific mechanism. Besides the deterioration of mass transport in the catalyst layer, which is usually assumed to be mainly responsible for voltage loss during start/stop cycling, an increased ionomer resistance and the formation of isolated electrode areas are suggested to significantly contribute to the strong decline in fuel cell performance.

Start-Stop Experimental Series at the Stack Level

These studies were carried out at the 'Berner Fachhochschule für Technik and Informatik' (BFH-TI) with single cells and stacks of the IHPoS-S Type. This fuel cell is a fully industrialized product from the company CEKAtec. The industrialization of the fuel cell stack was carried out within the scope of a CTI-Project in cooperation with the BFH-TI and the PSI.

The start-stop strategies developed within the framework of go.PEF-CH have been successfully implemented by the BFH-TI and CEKAtec in the IHPoS-E System. This system was developed in cooperation between CEKAtec, BFH-TI and the PSI within the scope of another CTI-Project which followed the previously mentioned one.

In addition to the above results, the knowledge generated is of importance on the one hand when designing a fuel cell stack and on the other hand for its integration, choice of operation mode in a fuel cell system as well as for calculations of profitability of a complete fuel cell solution for specific applications.

Experiments

One of the main tasks of the BFH-TI was to transfer the findings obtained at single cell level at PSI to the stack level, taking into account the limitations given by a real fuel cell system. The start stop procedure has been optimized for a CEKAtec IHPoS-E fuel cell system. To induce the ageing effects and to test the start/stop procedure, the fuel cell stack was subjected to a minimum of 1000 start/stop cycles. Each cycle is divided in four phases, starting and ending with the "stack off" mode, i.e. a potential-free state where the anodic and cathodic chambers are filled with air. In order to avoid degradation phenomena that occur when the cells are at OCV (open circuit voltage), a resistance *R* was connected to the stack.

Procedure:

- Phase 1 (Start): The anode is flooded with hydrogen to build-up the stack voltage. Resistor *R* is connected to the stack.
- Phase 2 (Operation): the stack is put under load to reach the nominal operating temperature; electrical and thermal energy as well as water are produced.
- Phase 3 (Stop): the anode is purged with air to remove the hydrogen from the stack, hereby transferring the stack in a potential-free mode. As in phase 1 the fuel cell is connected to a resistor *R*.
- Phase 4 (Cool down / Off): the stack cools down. During this phase the resistor *R* remains connected.

This cycle was repeated on the test bench to accelerate the aging of the cells, hereby monitoring the individual cell voltages as a measure for the 'state of health' and degradation of the cell components.

The following relevant parameters were studied:

- Duration of the purge time: optimum at ca. 12 s for start and stop
- Maximum air purge flow: optimum at 1 Ln/min per cell.
- Magnitude of resistor *R*: optimum at 0.5 Ohm per cell

The studies were carried out with a 10-cell and a 6-cell IHPoS-S Stack, respectively. The maximum air purge flow per cell and the auxiliary resistance *R* per cell correspond to those used in the fuel cell system IHPoS-E.

Results

Relevant for the investigations carried out in the fuel cell stack are phases 1 and 3 as described above. By optimizing the parameters in both phases, the lifetime of a stack can be significantly enhanced. This is because as the hydrogen (phase 1, hydrogen flooding of the anode filled with air) or air (phase 2, air purge of the anode filled with hydrogen) enters the anode of the fuel cell, a coexistence of hydrogen and air develops at the anode, inducing electrochemical reactions that cause degradation of the cathode components. The results of the degradation of the individual cells as a function of their position in the stack are shown in Figure 9. The voltage degradation of an individual cell is strongly related to its position within the stack. The cells closer to the gas inlets exhibit lower voltage losses. This phenomenon cannot be eliminated by changing flow rates or times during phase 1 and 3.

The maximum performance degradation after 1000 cycles obtained under the studied parameters was around 5%. The dependency of the degradation rate of the cells on their position relative to the gas inlet in the 10-cell stack has been corroborated in a 30-cell stack. The 30-cell stack is integrated in a IHPoS-E system. Figure 10 shows the individual cell voltages of the stack. A clear trend can be ob-

served: cells closer to the gas inlets (cell 1) show a higher operating voltage, while cells at the farther end (cell 30) show a lower voltage. Therefore, the degradation rate of cells farther from the gas inlets is higher.

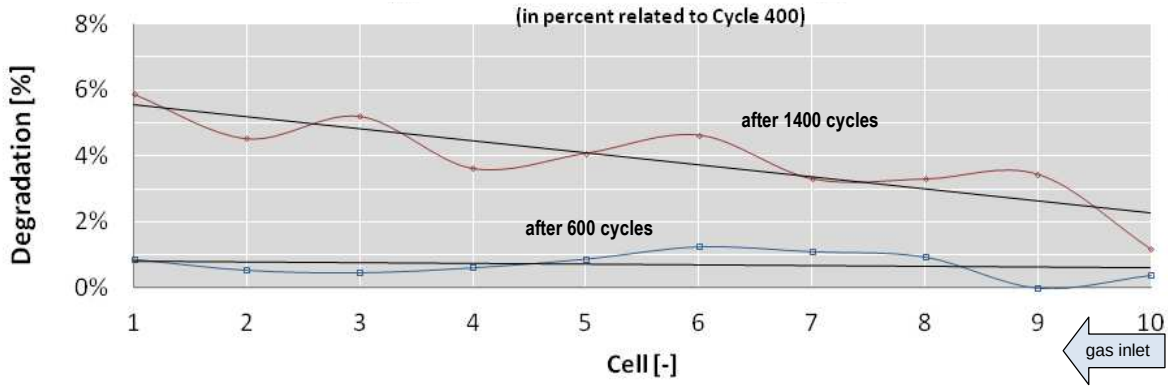

Figure 9 Degradation of individual cells as a function of their position in the stack. Cell No. 10 is the closest one to the gas inlets. The degradation is expressed in % of the voltage differences between Cycle 400[1] ("Beginning of life") and Cycles 600 and 1400, respectively. The voltage of the cells after different cycles was measured at a stack current of 17.5 A (~0.28 A/cm^2).

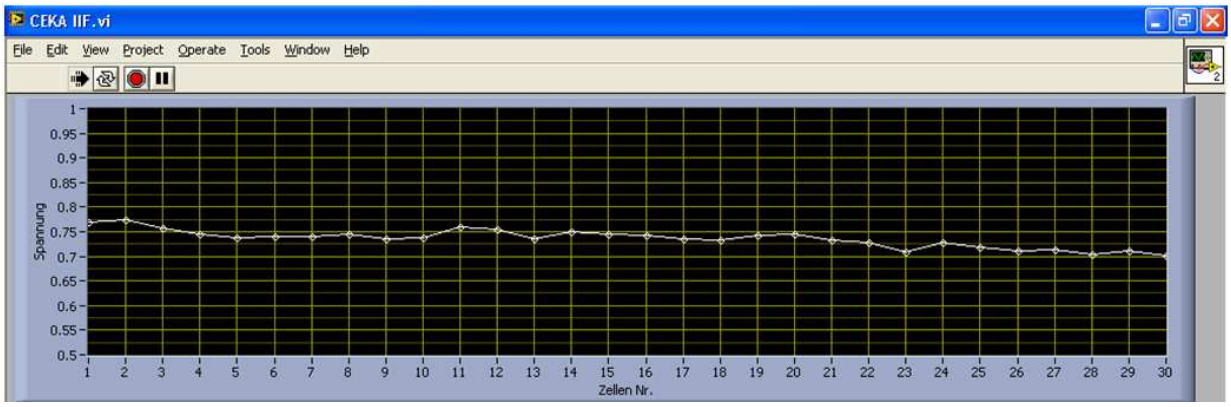

Figure 10 Screen shot from CEKAtec's test bench. The graph shows the individual cell voltages of the 30 cells in the stack. Cell Nr. 1 is the closest one to the gas inlets. The voltage of the single cells was measured at a stack current of 17.5A (~0.28 A/cm^2).

In addition to the above presented results, interesting findings in cell voltage behavior were obtained while monitoring single cell voltages during phase 1 and 3 of the cycling experiments.

Phase 1, Start.

The following time – cell voltage relationships can be seen on Figure 11.

- Time 0s:
  The Stack is off, i.e. both anode and cathode compartment are filled with air. Resistor *R* is connected.
- Time 1s-6s, Residual hydrogen effect:
  In order to transport condensed water out of the channels of the cells, both, anode and cathode are purged with air. During this phase it is interesting to see that, even though the stack and single cells show no potential before starting the procedure, and only air is pumped into the cells on both sides, single cells show voltage variations in the range of a few 10 mV. The potential of some cells turns positive while others show a reversed polarity. The positive potential might be attributed to residual hydrogen in the porous gas diffusion layer (GDL) of the anode electrode. The cells without residual hydrogen become either negative immediately or they do so after a certain period of time after the residual hydrogen is consumed (in comparison to other cells with higher residual hydrogen concentrations). This is because a resistor *R* is connected to the stack during the time at which

[1] cycle Nr. 400 was taken as the reference point, i.e. beginning of life because during the first 399 cycles the in- and outlet connectors of the hydrogen were connected in a wrong way.

the stack is purged with air. Therefore, those cells containing residual hydrogen produce electrical current, and those cells without hydrogen change polarity in order to sustain the current flowing through the stack.

- Time 6s-12s, flooding of the anode with hydrogen:
  The hydrogen valve is opened. Hydrogen enters the first cell (Nr. 10), raising its potential. Due to the series connection of the cells the current produced (due to the connected *R*) in the first cells leads to a voltage drop e.g. reverse polarity in the last cells since the introduction of hydrogen into these cells is delayed (red circle).

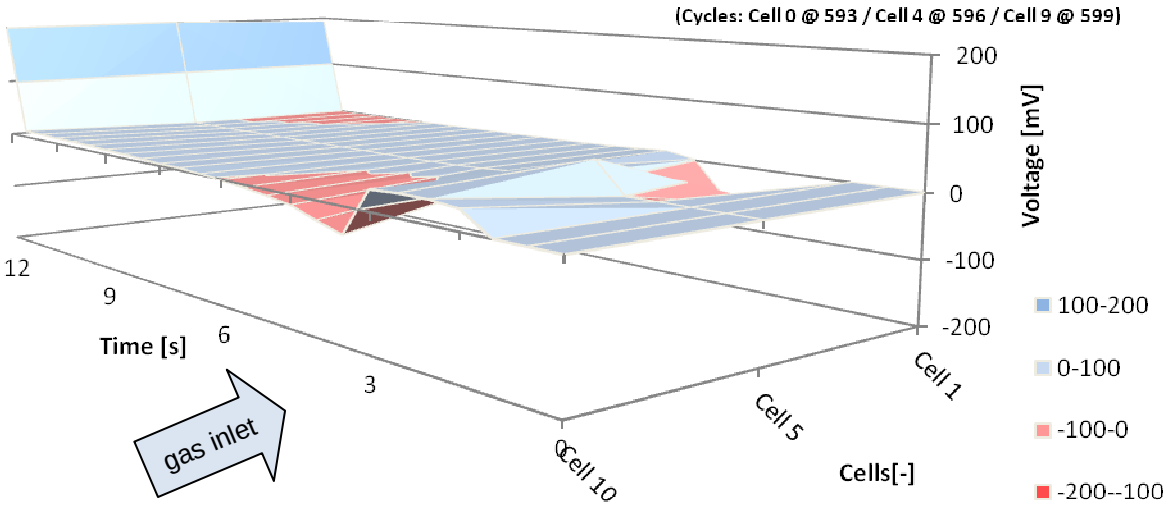

Figure 11 Changes in Individual cell voltage during the start process. For a better overview, only cells 1, 5 and 10 are shown. Cell 10 is the closest one to the gas inlet. Time axis goes from right to left.

- Phase 3, Stop:
  The individual cell voltage behavior when purging the hydrogen out of the cells with air can be observed in Figure 12. When purging the hydrogen out of the anode of the individual cells a similar but reverse effect can be observed. The cells closest to the gas inlet change polarity. This is because the cells farther away, still filled with hydrogen, produce electrical current due to the connected resistance *R*. The first seconds of the stop procedure lead to a change in cell polarity in the first cells. However, after a few seconds their polarity changes to positive and the cells further away from the gas inlet show a negative potential. This effect cannot yet be explained. Nevertheless, the changes in polarity are in the range of a few 10 mV and are not expected to affect the time of life of the cells in a critical manner.

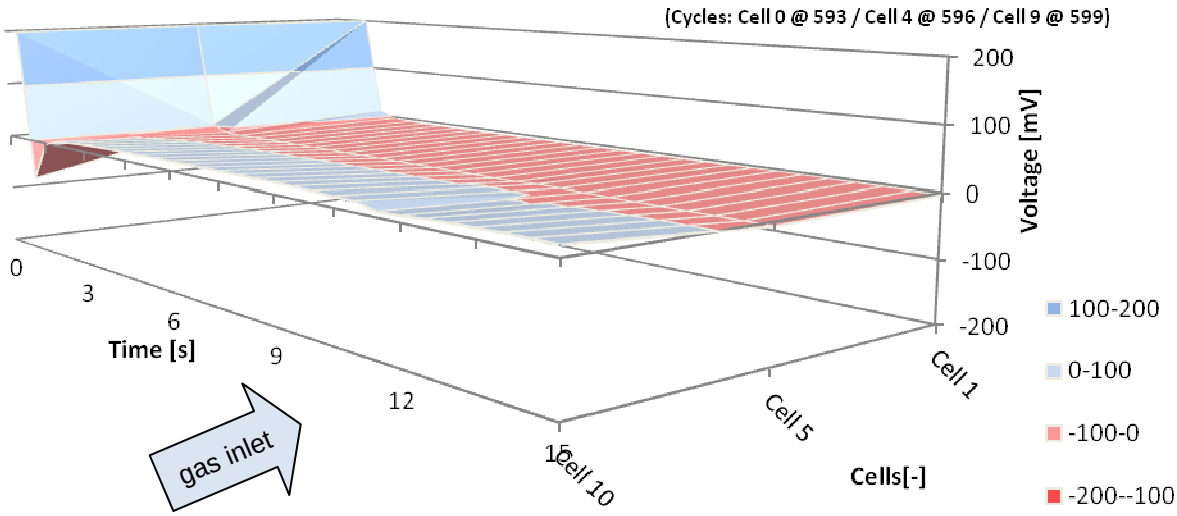

Figure 12 Changes in Individual cell voltage during the stop process. For a better overview, only cells 1, 5 and 10 are shown. Cell 10 is the closest one to the gas inlet. Time axis goes from left to right for a better overview.

Outlook

There is still work to do within the scope of enhancing the time of life of the IHPoS-S Stack. Further experimental series need to be carried out in order to corroborate the findings and to implement possible strategies to minimize the inhomogeneous aging of the cells. Taking into consideration the financial implications of experiments with the aim of studying aging phenomena, tests can be carried out with minimal need for new components for each set of tests. Furthermore, some tests can be carried out in a straightforward manner without the need for additional hardware changes.

Examples:

- Changing the cell position in relation to the gas inlets; e.g. first cell or cell-group is transferred to the far end of the stack and vice-versa after a certain number of cycles.
- With hardware modifications:
  Changing the position of the gas inlets relative to the cells; e.g. gas-connectors in the center of the stack.
- Modeling work:
  Modeling work could be carried out in order to better understand the fluid-dynamics implications during the start/stop procedures. Thereby, results which could support the optimization of the cell-geometries could be generated. Also applying a resistor *R* to each single cell could be part of the modeling work.

Start/Stop at temperatures below 0℃:

One of the main restrictions for PEM fuel cells when used in real life applications is the degradation of cell components when storing a fuel cell stack at temperatures below the freezing point. Applying the experimental methods used to carry out the work reported here and, more importantly, the generated know-how to this set of yet unsolved problems would be of great importance for helping to realize a wider set of specific application with such demands for a fuel cell system.

TRANSIENT PHENOMENA IN SELF-HUMIDIFYING POLYMER ELECTROLYTE FUEL CELLS

Good progress could be made in 2011 in novel investigations of convective mass flow between two adjacent flow field channels. The results have been made within this project can be seen as important cornerstones for improvements of the local performance as well as local degradation. Spatially resolved measurements in both directions, along the channel and in channel and land areas scrutinize several weak points of the MES S.A. fuel cell stack. This paves the way to performance and lifetime enhancements.

Investigation of the short circuit system for self-humidification of the fuel cell stack

One important issue is the investigation of the short circuit system. For self-humidification, the fuel cell stack of MES S.A. is short-circuited with a power MOSFET every 20 s for 50 ms each. This system enhances the performance of the fuel cell stack by 20-30% due to formation of product water with just a minor negative effect on the durability. However, to investigate the effects of the self-humidification system, local transients of the current density and high frequency distribution are measured.

The behavior of the fuel cell stack operated in the default mode with the software of MES S.A. is shown in Figure 13. An integral current of 30 A is drawn by an external load. The local current densities in the *along the channel* direction and the cell voltage are displayed in Figure 13a. Here, the short circuits are clearly noticeable at t = 1 s and t = 21 s. For a better discussion, in Figure 13b a time interval of 0.3 s around a short circuit is shown. Between t = 1.005 s and t = 1.055 s the stack is short-circuited with a power MOSFET. As a consequence, the local current densities step to values of more than i = 5 A/cm^2. Meanwhile, the cell voltage decreases to about U = 70 mV. Note here, that the short circuit system with the power MOSFET behaves not like an ideal conductor and therefore the voltage does not approach U = 0 V. During the 50 ms period of the short circuit, the local current densities decrease to values of i = 2 A/cm^2. This behavior is ascribed to the electroosmotic drag of water molecules from the anode to the cathode electrode, which dries out the anode [8, 9]. After the short circuit, the voltage and the local current densities recuperate. A closer insight gives the measurement of the local high frequency resistance (HFR, measured at f = 1 kHz), shown in Figure 13c. Apart from an offset value, the behavior of the HFR is similar for all segments in the *along the channel* direction. An interesting finding is here, that 1-2 s after the short circuit, the values are very close to those values before the short circuit. Even at t = 1.1 s, which is about 50 ms after the short circuit, the HFR is less than 5 % smaller compared to t = 0.9 s, which is about 100 ms before the short circuit (Figure 13d). However, the current density is up to10 % higher and as already mentioned, in the long term the performance of the stack is 20-30% better.

The shape of the current density as well as the high frequency resistance distribution in the along the channel direction originates from the gas supply of the stack, which is operated in counter flow mode. The hydrogen inlet is at segment 1, the air inlet at segment 8. In principle, the resistance is elevated at both gas inlets, due to the supply with non-humidified gases. Obviously, in this operation mode (integral current of 30 A) the current density is primarily controlled by the high frequency resistance. The minimum in the current density and the maximum in the high frequency resistance in the region of segment 5 and 6 originate from a change in the flow field. At the air inlet (segment 6-8), broader lands prevent the cell from drying out.

Investigation of the short circuit system for self-humidification of the fuel cell stack

Another key experiment is the investigation of transients occurring during the start-up and the shut-down procedure of the stack. The local current densities of one cell over the whole time period of both procedures are shown in Figure 14a. During a start-up procedure, a preliminary phase of test is done. At the point denoted with α (t = 19.2 s), the hydrogen valve is opened, so that hydrogen penetrates the anode compartment of the cells. For 100 ms no additional actions are done in order to permit the hydrogen to reach all the cells. The local current densities during the hydrogen penetration of one cell are shown in Figure 14b. High local currents of up to 1 A/cm^2 were measured, although no integral current was drawn by the stack. As expected, during the start-up of the stack hydrogen first reaches segment 1. This causes a positive current in this segment and drives a negative current through the other hydrogen starved segments. In literature, these local currents emerging during start-up and shutdown of a PEFC are discussed as a source for degradation of the carbon catalyst layer [1, 10]. This phenomenon known as the reverse-current decay mechanism [1] might lead to severe cell degradation due to carbon corrosion in the catalyst layer. Therefore, it has been investigated more in de-

tail with the segmented microstructured flow field approach. A publication about the start-stop phenomena occurring on channel and land scale can be found in literature [11].

One common strategy to mitigate the detrimental carbon corrosion reactions is the reduction of the hydrogen introduction time during start-up [12, 13]. Complying with this mitigation strategy, in the stack of MES S.A., the gas front has passed the cell on a time scale of less than 10 ms. During the current transients, the voltage increases from U = 0 V to about U = 0.8 V.

After this hydrogen introduction phase and the mentioned interval of 100 ms, the stack voltage is kept under control by several short circuits for 2 seconds. This assures the complete filling of the anode compartment with hydrogen while the carbon corrosion phenomenon is additionally mitigated by the reduced voltage [14]. Thereby, since the gas supply at the cathode is not activated at this moment, the local current densities drop due to the consumption of the residual oxygen at the cathode.

The next step during the start-up procedure is the start of the air blower for cathode gas supply. This point is denoted with β (t = 24.2 s) in Figure 14a and shown more in detail in Figure 14c. As expected, here the transient moves from segment 8 to segment 1, since the air inlet is at segment 8 and there is a steep gradient of the oxygen concentration due to the consumption of the reactant gas during the previous phase. After the gas supply of both reactant gases is enabled, the external load is connected to the stack and draws an integral current of 30 A (I = 0.5 A/cm^2). This point is denoted with γ in Figure 14a (t = 29.2 s).

Just after a few seconds of operation, the shutdown process was manually started. During the shutdown procedure, the auxiliary systems of the fuel cell stack are operated in a way to decrease the stack voltage without the depletion of the hydrogen in the anode compartment in order to avoid any detrimental hydrogen starvation and attributed degradation phenomena. After the air blower is switched off, so that a major fraction of the oxygen in the cathode compartment is consumed, the shutdown procedure is completed by a short circuit. This short circuit denoted with δ in Figure 14a (between t = 67.09 s and t = 67.14 s) is shown in detail in Figure 14d. The transients are similar to those of the short circuits of the self-humidifying system (Figure 14b), although the current densities are significantly smaller, possibly due to the lower oxygen concentration. This is also expected as the reason for a rather slow increase of the voltage, which in fact mitigates detrimental high cell potentials.

Effect of Convective Channel-to-Channel Mass Flow

Novel results gained in 2011 are on the convective channel-to-channel mass flow [15]. Since a parallel flow field is employed in the MES S.A. stack and therefore no convective mass flow is generated by this flow field design, the results are encouraging to reconsider the design.

The effect of convective channel-to-channel mass flow on the local performance of a polymer electrolyte fuel cell (PEFC) air cathode is determined experimentally by using submillimeter resolved current density distribution measurements in channel and land areas. A special cell is employed, where the two parallel channels of the cathode flow field can be operated at different pressure. For isobaric operation of the channels (Δp = 0 mbar), the lateral current density distribution shows a distinct minimum in the land area between the channels as diffusive mass transport becomes limiting at a higher cell polarization (Figure 15). Toward higher Δp, the local cell performance in the land area improves initially as a result of an improving convective channel-to-channel mass flow. However, as the pressure difference exceeds a value of 10 mbar, no noteworthy additional benefit is observed with further increasing Δp (Figure 15). Under these conditions, the convective mass flow provides an abundant reactant supply in the land area and, since reactant depletion is no longer limiting, the lateral current density distribution is primarily governed by the local ohmic resistance. As a result, the current density exhibits a maximum in the land area, where the local ohmic resistance shows a minimum.

A sufficient reactant supply is a fundamental requirement for an efficiently operating fuel cell and paves the way to reduce the Pt expenditure. This can bring lower unit costs and furthermore an enhanced power density of a PEFC. The results presented in this work demonstrate that the optimization of the flow field plates is an important factor for an efficient utilization of the catalyst particles. It was proven that the reactant supply in the land area is a critical issue. Here, convective mass flow can improve the reactant transport underneath the land area, which is induced by a pressure difference Δp between two adjacent flow channels. In this work, the effect of the pressure difference Δp on the local cell performance could be determined for the first time experimentally. Even small pressure differences of Δp = 2 mbar between two adjacent flow field channels improve the mass transport in the land area. At large channel-to-channel pressure differences of Δp > 10 mbar, a differential mass flow is achieved underneath the land and reactant depletion becomes negligible. Under these conditions, the

local current density distribution is governed by the local ohmic resistance and with the employed flow field an impressive performance gain of 70% was obtained. The method presented in this work can be used to examine the effect of the pressure difference Δ*p*, different GDL materials and various channel and land widths on the local performance in the land area. Key parameters required for the flow field development can be experimentally determined.

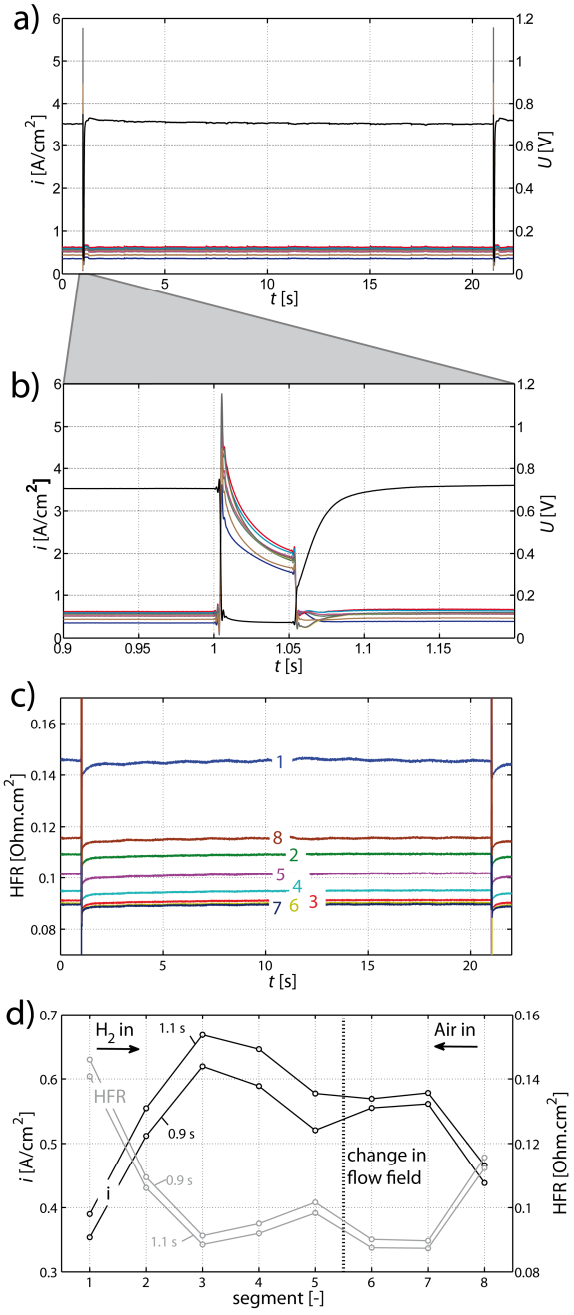

Figure 13. a) Local current densities and voltage of one cell in the fuel cell stack of MES S.A. during operation with the short circuit system ($I_{integral}$ = 30 A, operated with the software of MES S.A.), b) local current density and voltage in a time interval of 0.3 s around a short circuit, c) local high frequency resistance and d) current density and high frequency distribution for two distinct points close before and after a short circuit.

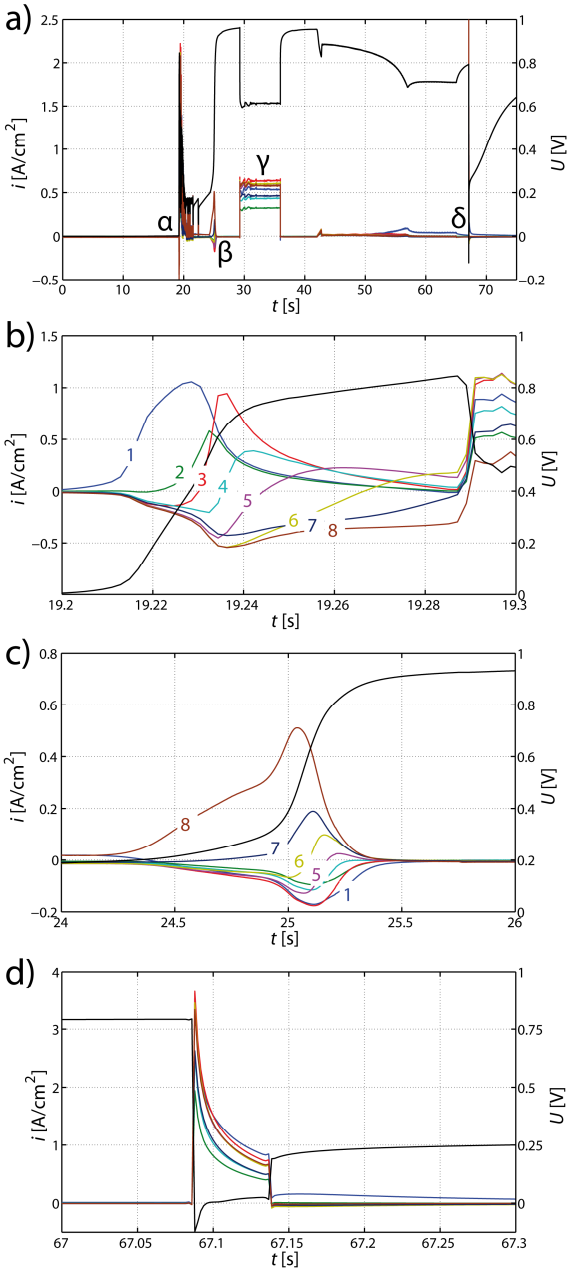

Figure 14. a) Local current densities and voltage of one cell in the fuel cell stack of MES S.A. during the time period of a start-up and a shutdown procedure, b) current and voltage transients during the hydrogen introduction (α), c) current and voltage transients during start of the air blower (denoted with β) and d) short circuit during the shutdown procedure (denoted with δ).

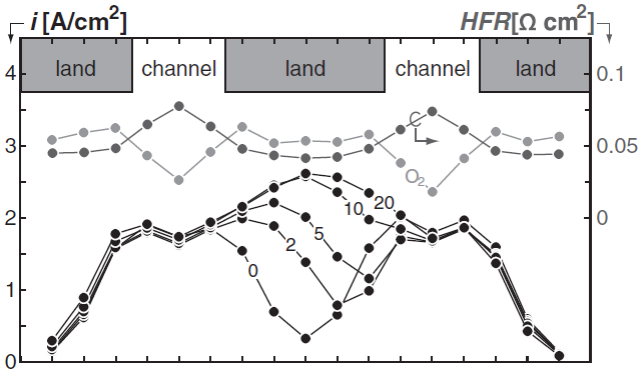

Figure 15. Local current densities in channel and land areas of a PEFC operated on a cell voltage of U = 0.3 V and Δp = 0-20 mbar. In grey: Measurements with oxygen instead of air (Δp = 0 mbar, f = 10 kHz) [15].

National Collaboration

– Cal.PEF-CH: Model based investigation of PE fuel cell performance with focus on porous layer properties
with ZHAW, Winterthur

– hy.muve: Development of hydrogen powered municipal vehicle
with EMPA Dübendorf and Industrial Partners

– PSI is collaborating with Belenos Clean Power Holding, which was founded in 2007, with the aim of developing a fuel cell powered car in the framework of a sustainable mobility concept involving also photovoltaics and water electrolysis.

International Collaboration

– In the area of fuel cell diagnostics, PSI is collaborating with a number of automotive companies (e.g. Nissan Motor Co.).

– In the area of diagnostics, PSI is collaborating with a fuel cell stack and system manufacturer in Canada.

Conferences & Publications

Peer reviewed publications

– Quantification of platinum deposition in polymer electrolyte fuel cell membranes
H. Schulenburg, B. Schwanitz, J. Krbanjevic, N. Linse, G. G. Scherer, A. Wokaun
Electrochemistry Communications 13 (2011) 921–923

– The effect of platinum on carbon corrosion behavior in polymer electrolyte fuel cells
N. Linse, L. Gubler, G.G. Scherer, A. Wokaun
Electrochim. Acta, 56, 7541-7549 (2011).

– 3D Imaging of Catalyst Support Corrosion in Polymer Electrolyte Fuel Cells
H. Schulenburg, B. Schwanitz, N. Linse, G.G. Scherer, A. Wokaun, J. Krbanjevic, R. Grothausmann, I. Manke
J. Phys. Chem. C 115, 14236–14243 (2011)

– Start-Stop phenomena in channel and land areas of a polymer electrolyte fuel cell
I.A. Schneider, S. von Dahlen
Electrochem. Solid State Lett. 14, B30-B33 (2011).

– Locally resolved electrochemical Impedance spectroscopy in channel and land areas of a differential polymer electrolyte fuel cell.
I.A. Schneider, M.H. Bayer, S. von Dahlen
J. Electrochem. Society 158, B343-B348 (2011)

– Local Transients of Flooding and Current in Channel and Land Areas of a Polymer Electrolyte Fuel Cell
I.A. Schneider, S. von Dahlen, M.H. Bayer, P. Boillat, M. Hiltebrandt, E.H. Lehmann, P. Oberholzer, G.G. Scherer, A. Wokaun
J. Phys. Chem. C 2010, 114, 11998-12002

– A Segmented Microstructured Flow Field Approach for Submillimeter Resolved Local Current Measurement in Channel and Land Areas of a PEFC
I. A. Schneider, S. von Dahlen, A. Wokaun, and G. G. Scherer
Journal of The Electrochemical Society, 157 (3) B338-B341 (2010)

– Local transient techniques in polymer electrolyte fuel cell (PEFC) diagnostics
I.A. Schneider, G.G. Scherer
Handbook of Fuel Cells – Fundamentals, Technology and Applications. Edited by Wolf Vielstich. Harumi Yokokawa, Hubert A. Gasteiger.
Volume 6,Chapter 45, 2009: Advances in Electrocatalysis, Materials, Diagnostics and Durability.
ISBN: 978-0-470-72311-1.

Conference Proceedings

– N. Linse, C. Aellig, A. Wokaun, G.G. Scherer, L. Gubler
Influence of operating parameters on start/stop induced degradation in polymer electrolyte fuel cells
ECS Transactions 25 (1) 1849-1859 (2009).

– N. Linse, G.G. Scherer, A. Wokaun, L. Gubler
Start/stop induced carbon corrosion in polymer electrolyte fuel cells
Proc. 8th Fuel Cell Science and Technology Conference ASME 2010, Fuel Cell 2010-33190, Brooklyn, New York, June 14-16 (2010).

– I.A. Schneider, S. von Dahlen, M.H. Bayer, G.G. Scherer, A. Wokaun
AC impedance and transient technique based PEFC diagnostics: Insights from submillimeter resolved local measurements in channel and land areas
ECS Transactions 33, 1321-1334 (2010).

– H. Schulenburg, B, Schwanitz, J. Krbanjevic, N. Linse, R. Mokso, M. Stampanoni, A. Wokaun, G.G. Scherer
3D Imaging of polymer electrolyte fuel cell electrodes
ECS Transactions 33, 1471-1481 (2010).

– S. von Dahlen, G.G. Scherer, A. Wokaun, I.A. Schneider
Start-stop phenomena in channel and land areas of a polymer electrolyte fuel cell (PEFC)
ECS Transactions 33, 1365 (2010).

Deliverable Status

Work Package 1 (Start / Stop Induced Degradation)

D1	*WP1*	55 / 120 MEAs received so far **Deliverable 45% completed**, further components not required to meet project objectives
D2	*WP1.1*	IPHoS Hardware design finalized. Comparison of performance of 6-cell IPHoS stack at Biel and PSI carried out, indentical performance obtained **Deliverable 100% completed**
D3	*WP1.2*	Sub-scale cell hardware with 16 cm^2 active area commissioned and extensively used **Deliverable 100% completed**
D4	*WP1.3*	Major degradation effects identified, quantified and published **Deliverable 100% completed**
D5	*WP1.4*	Start / stop test over 1'400 cycles in IHPoS hardware completed and degradation

		quantified. **Deliverable 100% completed**
D6	*WP1.5*	Mitigation strategies implemented in start-stop test using 10-cell IHPoS stack. The steady degradation rate in principle allows prediction of performance loss over time. **Deliverable 100% completed**
D7	*WP1.6*	Study on *post mortem* analysis of catalyst layer completed and being published **Deliverable 100% completed**
D8	*WP1.7*	PhD thesis handed in **Deliverable 100% completed**

Work Package 2 (Transient Phenomena)

D9	*WP2*	MES-DEA to supply BFH-TI and PSI with components and hardware: 120 MEAs, 10 single cells and 2 stacks / systems of 500 W **Deliverable 80% completed (no MEAs required)**
D10	*WP2.1*	Major transient effects are identified **Deliverable 100% completed**
D11	*WP2.2*	Investigations of the local transients of current density and high frequency resistance distribution during short circuits as well as start-up and shutdown processes **Deliverable 100% completed**
D12	*WP2.3*	Correlation of observed local transients in the stack with other conducted model experiments **Deliverable 100% completed**
D13	*WP2.4*	Transient phenomena investigated in both in plane directions, the *along the channel* and *perpendicular to the channel* direction **Deliverable 100% completed**
D14	*WP2.5*	Analysis of the short circuit effects on possible aging/damages of the MEA. Improvements and mitigation strategies of current MES-DEA's procedure in which the short circuit procedure is used **Deliverable 70% completed**
D15	*WP2.6*	PhD thesis handed in **Deliverable 100% completed**

Work Package 3 (Coordination)

D16	*WP3.1*	Action plan for future project under discussion (to continue in January 2012) **Deliverable 50% completed**
D17	*WP3.2*	New project proposals not drafted yet **Deliverable 0% completed**

References

[1] C. A. Reiser, L. Bregoli, T. W. Patterson, J. S. Yi, J. D. Yang, M. L. Perry, T. D. Jarvi, Electrochemical and Solid-State Letters 8(6), 2005, A273

[2] Z. Y. Liu, B. K. Brady, R. N. Carter, B. Litteer, M. Budinski, J. K. Hyun, D. A. Muller, Journal of The Electrochemical Society 155(10), 2008, B979

[3] N. Linse, L. Gubler, G. G. Scherer, A. Wokaun, Electrochimica Acta 56(22), 2011, 7541-7549

[4] K. G. Gallagher, D. T. Wong, T. F. Fuller, Journal of The Electrochemical Society 155(5), 2008, B488

[5] N. Linse, C. Aellig, A. Wokaun, G. G. Scherer, L. Gubler, ECS Transactions 25(1), 2009, 1849-1859

[6] N. Linse, G. G. Scherer, A. Wokaun, L. Gubler, Proceedings of the ASME Eighth International Fuel Cell Science, Engineering and Technology Conference, FUELCELL2010-33190, 2010

[7] H. Schulenburg, B. Schwanitz, N. Linse, G. G. Scherer, A. Wokaun, J. Krbanjevic, R. Grothausmann, I. Manke, The Journal of Physical Chemistry C 115(29), 2011, 14236-14243

[8] I. A. Schneider, and G. G. Scherer, in *Handbook of Fuel Cells*, Vol. 6, W. Vielstich, H. A. Gasteiger, and H. Yokokawa, Editors, John Wiley & Sons, New York, 2009

[9] Y. Wang, C. Y. Wang, *Electrochim. Acta*, 51, 2006, 3924

[10] A. P. Young, J. Stumper, E. Gyenge, J. Electrochem. Soc., 156, 2009, B913

[11] I. A. Schneider and S. von Dahlen, *Electrochem. Solid State Lett.*, 14 (2), 2011, B30-B33

[12] B. Wetton, R. Bradean, and K. Eggen, *Proceedings of the 20th International Symposium on Transport Phenomena*, 7-10 July, 2009, Victoria BC.

[13] W. Gu, R. N. Carter, P. T. Yu, and H. A. Gasteiger, *ECS Trans.*, 11 (1), 2007, 963

[14] J. P. Meyers, and R. M. Darling, *J. Electrochem. Soc.*, 153, 2006, A1432

[15] S. von Dahlen, M. H. Bayer, I. A. Schneider, *Electrochem. Commun.*, 14, 2011, 55